J Mol Model (2007) 13:927–935
DOI 10.1007/s00894-007-0210-y

ORIGINAL PAPER

Structures and aromaticity of Cationic *closo*-$B_nH_{n-3}(CO)_3^+$ (n=5−12)

Xiao-Fang Qin · Hai-Shun Wu · Haijun Jiao

Received: 27 December 2006 / Accepted: 23 April 2007 / Published online: 5 June 2007

Abstract Structures and stabilities of tricarbonyl *closo*-boranes cation, $B_nH_{n-3}(CO)_3^+$ (n=5−12), isolobal with cationic *closo*-carboranes $C_3B_{n-3}H_n^+$, have been investigated at the B3LYP/6−311+G** level of theory. The most stable positional isomers of individual cluster are in agreement with those of *closo*-$C_3B_{n-3}H_n^+$ clusters except for n=8 and 10. Energetic analysis identifies *closo*-$B_6H_3(CO)_3^+$, *closo*-$B_{10}H_7(CO)_3^+$ and *closo*-$B_{12}H_9(CO)_3^+$ as the most stable cages. It is also found that *closo*-$B_nH_{n-3}(CO)_3^+$ is much less strained than *closo*-$C_3B_{n-3}H_n^+$. The negative nucleus independent chemical shifts (NICS) at the cage center reveal three-dimensional aromaticity of the *closo*-$B_nH_{n-3}(CO)_3^+$ cages. The CO stretching frequencies have been computed in advance to aid experimental study.

Keywords Aromaticity · DFT · Stability · Tricarbonyl *closo*-boranes cation

Electronic supplementary material The online version of this article (doi:10.1007/s00894-007-0210-y) contains supplementary material, which is available to authorized users.

X.-F. Qin · H. Jiao (✉)
State Key Laboratory of Coal Conversion, Institute of Coal chemistry, Chinese Academy of Sciences,
Taiyuan 030001, People's Republic of China
e-mail: haijun.jiao@catalysis.de

H.-S. Wu
School of Chemistry and Materials Science,
Shanxi Normal University,
Linfen 041004, People's Republic of China
e-mail: wush@dns.sxnu.edu.cn

H. Jiao
Leibniz-Institut für Katalyse e.V. an der Universität Rostock,
Albert-Einstein-Strasse 29a,
Rostock 18059, Germany

Introduction

Closo-$C_2B_{n-2}H_n$, formed by replacing two BH groups of $B_nH_n^{2-}$ by two CH^+ groups, and isolobal as well as isoelectronic to *closo*-$B_nH_n^{2-}$, is a widely studied class of carbon-containing polyhedral boron clusters [1–3]. The relative stabilities of the positional isomers of *closo*-$C_2B_{n-2}H_n$ (n=5−12) have been studied at various levels of theory [4–7]. The replacement of three BH groups of $B_nH_n^{2-}$ by three CH^+ groups leads to the positively charged carbon rich carboranes $C_3B_{n-3}H_n^+$. Jemmis et al. computed these carbon clusters, $C_3B_{n-3}H_n^+$ (n=5, 6, 7, 10, 12), [8] and found that the most stable isomers have the largest number of B-C bonds and obey the rule of maximum ring-cap orbital overlap. The $C_3B_{n-3}H_n^+$ stability increases with increased cage size. The spherical distribution of the positive charge makes these clusters suitable candidates as weakly electrophillic cations.

The isolobal analogy [9] of the $^4\Sigma^-$CH excited state and the $^4\Sigma^-$BCO ground state [10, 11] has found wide applicability. For example, the 1937 prepared H_3BCO [12] is isolobal with CH_4, and the recently observed OCB≡BCO [13] is the HC≡CH equivalent. Further examples are monocyclic boron carbonyl compounds $(BCO)_x^y$ with 4n+2 delocalized π electrons, [14] which are isolobal with the corresponding aromatic hydrocarbon species $(CH)_x^y$. However, the isolobal $(CH)_n$ and $(BCO)_n$ polyhedral cages differ strongly in structure and stability [15]. For example, $(BCO)_n$ cages are much less strained than the $(CH)_n$ analogs, and the most stable $(BCO)_n$ ($n \geq 10$) prefer structures with the largest number of three-membered rings, while $(CH)_n$ prefers cages with five- and six-membered rings. This isolobal relationship also has been applied to positively charged boron carbonyls, i.e., H_4BCO^+ is isolobal with CH_5^+, $(BCO)_2H^+$ is isolobal with the bridged

vinyl cation $C_2H_3^+$, $(BCO)_2C_5H_9^+$ is isolobal with 2-norbornyl cation and $(BCO)_5^+$ is isolobal with $(CH)_5^+$ [16]. It is found that the BCO analogs have geometries and electronic structures similar to those of their carbocation counterparts.

Replacing three CH groups of *closo*-$C_3B_{n-3}H_n^+$ by three BCO groups results in the isolobal tricarbonyl *closo*-boranes cation, *closo*-$B_nH_{n-3}(CO)_3^+$. Due to the unusual stability and the promising application of the cationic carborane systems as weakly electrophillic cations, it is interesting to know whether *closo*-$B_nH_{n-3}(CO)_3^+$ has the same relative stability as *closo*-$C_3B_{n-3}H_n^+$. In addition, we are interested also in the cage stability and aromaticity of *closo*-$B_nH_{n-3}(CO)_3^+$.

Computational details

All structures reported were optimized at the B3LYP/6−311+G** level of density functional theory, and characterized as energy minimum structures by frequency calculations at the same level. Frequency calculations provide also zero-point energies (ZPE). All relative energies were calculated at the B3LYP/6−311+G** level including the correction of ZPE (scaled by an empirical factor of 0.990 at the B3LYP/6−311+G** level).

As a simple and efficient criterion of aromaticity, nucleus independent chemical shifts (NICS), [17–19] the negative of the computed absolute shielding at the cage center, were used to characterize the aromaticity of these cages. The NICS values were computed at B3LYP/6−311+ G** by using the gauge-independent atomic orbital (GIAO) [20] method and the B3LYP/6−311+G** geometries. In addition to the structure, stability and aromaticity, we have calculated CO stretching frequencies to aid experimental investigations. All calculations were carried out with the Gaussian 03 program [21]. The computed total electronic energies, the zero-point energies and CO stretching frequencies are given in Supporting Information.

Results and discussion

(a) **Geometries and stabilities**: *Closo*-$B_nH_{n-3}(CO)_3^+$ has the same polyhedral structural pattern and the same number of positional isomers as c*loso*-$C_3B_{n-3}H_n^+$. The optimized structures are shown in Fig. 1 and the relative energies are given in Table 1. For direct comparison the relative energies for *closo*-$C_3B_{n-3}H_n^+$ at the B3LYP/6−31G* level are given in Table 1. Since Jemmis et al. have reported only $B_nH_{n-3}(CO)_3^+$ (n=5, 6, 7, 10, 12), [8] we have completed n=8, 9, and 11 at the same level of theory for fully comparison.

There are several qualitative approaches available to predict and rationalize the relative stabilities of positional isomers within a given polyhedral system. In one approach, Williams [22, 23] suggested that the CH groups prefer to occupy the vertices with the lowest connectivity to the neighboring nuclei resulting in the relative stability of all positional isomers of *closo*-dicarboranes. In another approach, the topological charge stabilization rule of Gimarc [24] states that the positions of the heteroatoms (e.g., CH) in a structure prefer the site with the largest negative charge in the isoelectronic borane system. Gimarc has used this empirical rule to successfully explain the relative stabilities of *closo*-carboranes. A third qualitative approach involves the idea of the compatibility of orbital overlaps by Jemmis, [25] and this was used previously to explain the relative stabilities of polyhedral carboranes.

Closo-$B_5H_2(CO)_3^+$ (**1a–1c**): As shown in Fig. 1, there are three isomers for *closo*-$B_5H_2(CO)_3^+$, i.e., **1a** in D_{3h} symmetry, **1b** in C_s symmetry and **1c** in C_{2v} symmetry. The most stable isomer is **1c**, while **1a** and **1b** are higher in energy by 4.4 and 5.4 kcal mol^{-1}, respectively. It is to note that **1c** has the smallest connectivity of the BCO groups and the largest separated negative charge at B1 and B5 positions.

Closo-$B_6H_3(CO)_3^+$ (**2a–2b**): There are only two isomers for *closo*-$B_6H_3(CO)_3^+$, i.e.; **2a** in C_{3v} symmetry and **2b** in C_{2v} symmetry. **2b** is more stable than **2a** by 2.8 kcal mol^{-1}. Although **2a** and **2b** have the same connectivity, **2b** has a larger separated negative charge at B1, B2, and B6. Therefore, the higher stability of **2b** is expected.

Closo-$B_7H_4(CO)_3^+$ (**3a–3e**): Five isomers for *closo*-$B_7H_4(CO)_3^+$ are found; i.e., **3a** in C_{2v} symmetry, **3b** and **3c** in C_s symmetry, as well as **3d** and **3e** in C_{2v} symmetry. The most stable isomer is **3e**, and the other isomers are higher in energy by 15.1 (**3a**), 14.7 (**3b**), 5.7 (**3c**) and 9.3 (**3d**) kcal mol^{-1}. As given in Table 1, the BCO groups in **3e** have the least connectivity and the largest separated negative charge at B2, B4 and B6 positions.

Closo-$B_8H_5(CO)_3^+$ (**4a–4i**): Nine isomers are found for *closo*-$B_8H_5(CO)_3^+$, i.e., **4a–4d**, **4g** and **4h** in C_s symmetry, and **4e**, **4f** and **4i** in C_1 symmetry. The most stable isomer is **4e**, tightly followed by **4h** (0.3 kcal mol^{-1}). The other isomers are higher in energy by 16.2 (**4a**), 11.3 (**4b**), 15.6 (**4c**), 10.5 (**4d**), 10.5 (**4f**), 16.4 (**4g**) and 8.1 (**4i**) kcal mol^{-1}. Although **4h** has less connectivity than **4e**, but **4e** has the largest separated negative charge. Nevertheless, this energy difference is too small for any quantitative comparison.

Fig. 1 Optimized structures and the natural charge on B atom of the BCO groups for *closo*-$B_nH_{n-3}(CO)_3^+$ (n=5−12) ▶

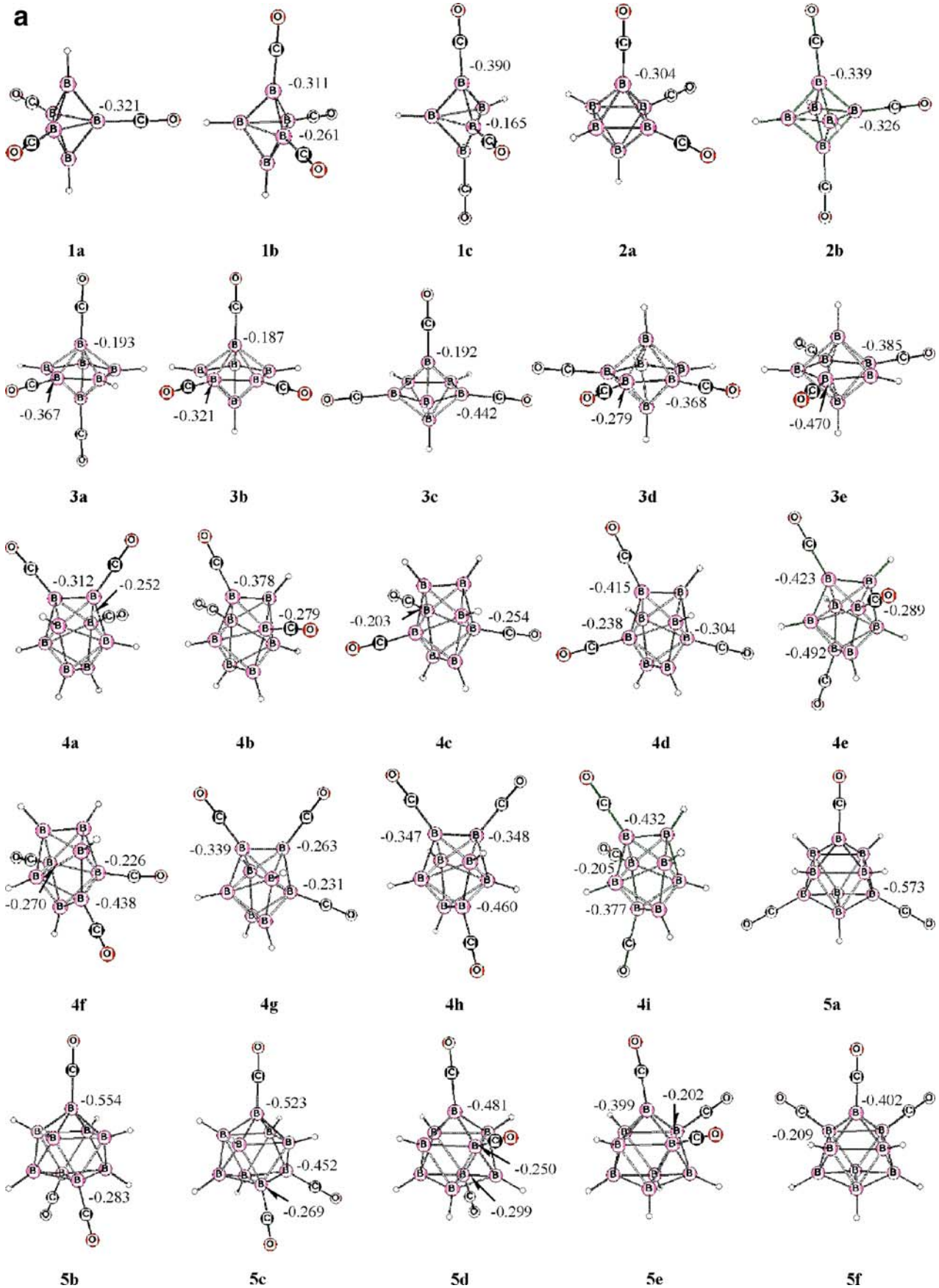
a
-0.321
1a
-0.311
-0.261
1b
-0.390
-0.165
1c
-0.304
2a
-0.339
-0.326
2b
-0.193
-0.367
3a
-0.187
-0.321
3b
-0.192
-0.442
3c
-0.279
-0.368
3d
-0.385
-0.470
3e
-0.312
-0.252
4a
-0.378
-0.279
4b
-0.203
-0.254
4c
-0.415
-0.238
-0.304
4d
-0.423
-0.289
-0.492
4e
-0.226
-0.270
-0.438
4f
-0.339
-0.263
-0.231
4g
-0.347
-0.348
-0.460
4h
-0.432
-0.205
-0.377
4i
-0.573
5a
-0.554
-0.283
5b
-0.523
-0.452
-0.269
5c
-0.481
-0.250
-0.299
5d
-0.399
-0.202
5e
-0.402
-0.209
5f

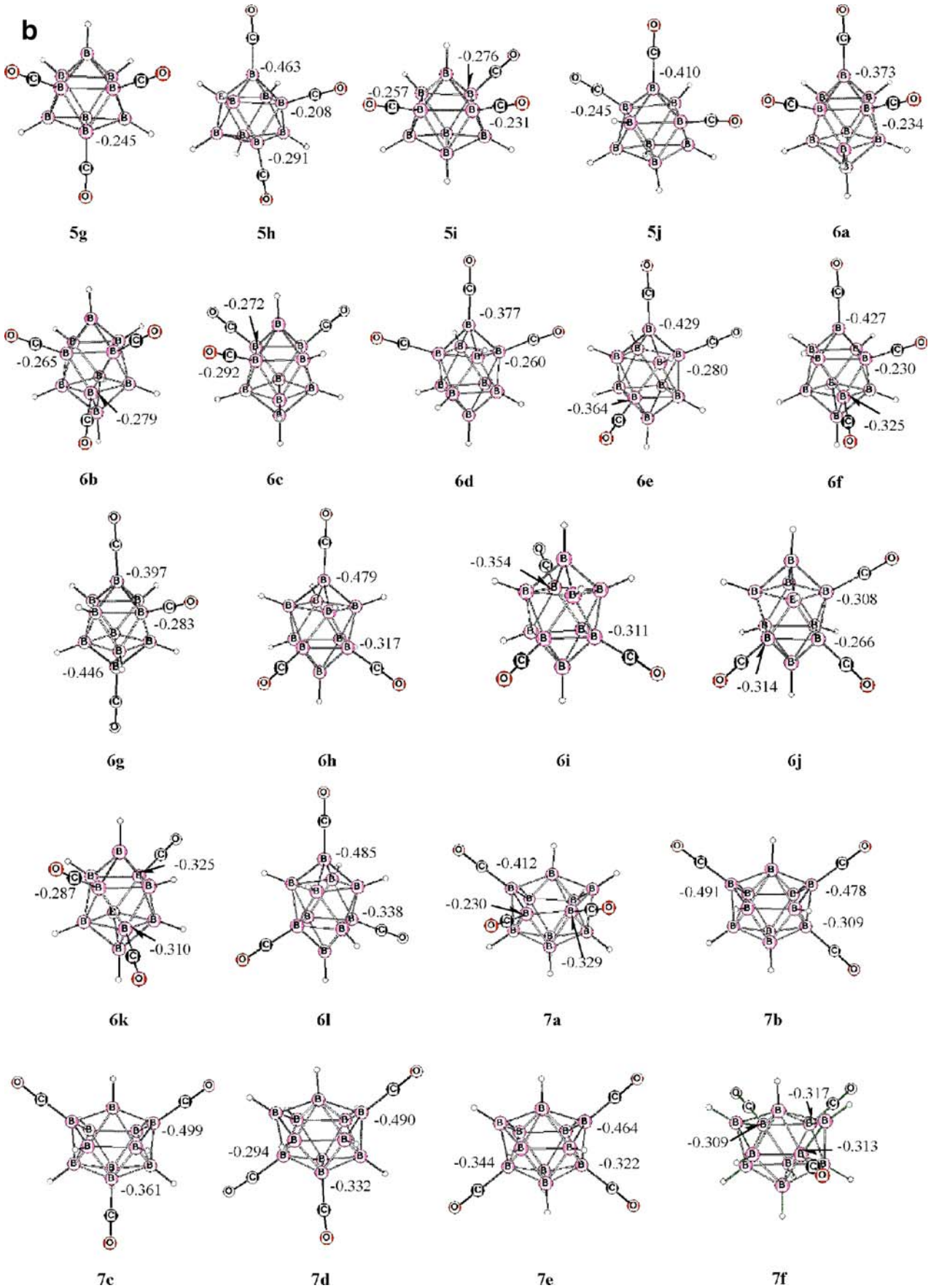
b
-0.245
5g
-0.463
-0.208
-0.291
5h
-0.276
-0.257
-0.231
5i
-0.410
-0.245
5j
-0.373
-0.234
6a
-0.265
-0.279
6b
-0.272
-0.292
6c
-0.377
-0.260
6d
-0.429
-0.280
-0.364
6e
-0.427
-0.230
-0.325
6f
-0.397
-0.283
-0.446
6g
-0.479
-0.317
6h
-0.354
-0.311
6i
-0.308
-0.266
-0.314
6j
-0.325
-0.287
-0.310
6k
-0.485
-0.338
6l
-0.412
-0.230
-0.329
7a
-0.491
-0.478
-0.309
7b
-0.499
-0.361
7c
-0.490
-0.294
-0.332
7d
-0.464
-0.344
-0.322
7e
-0.317
-0.309
-0.313
7f

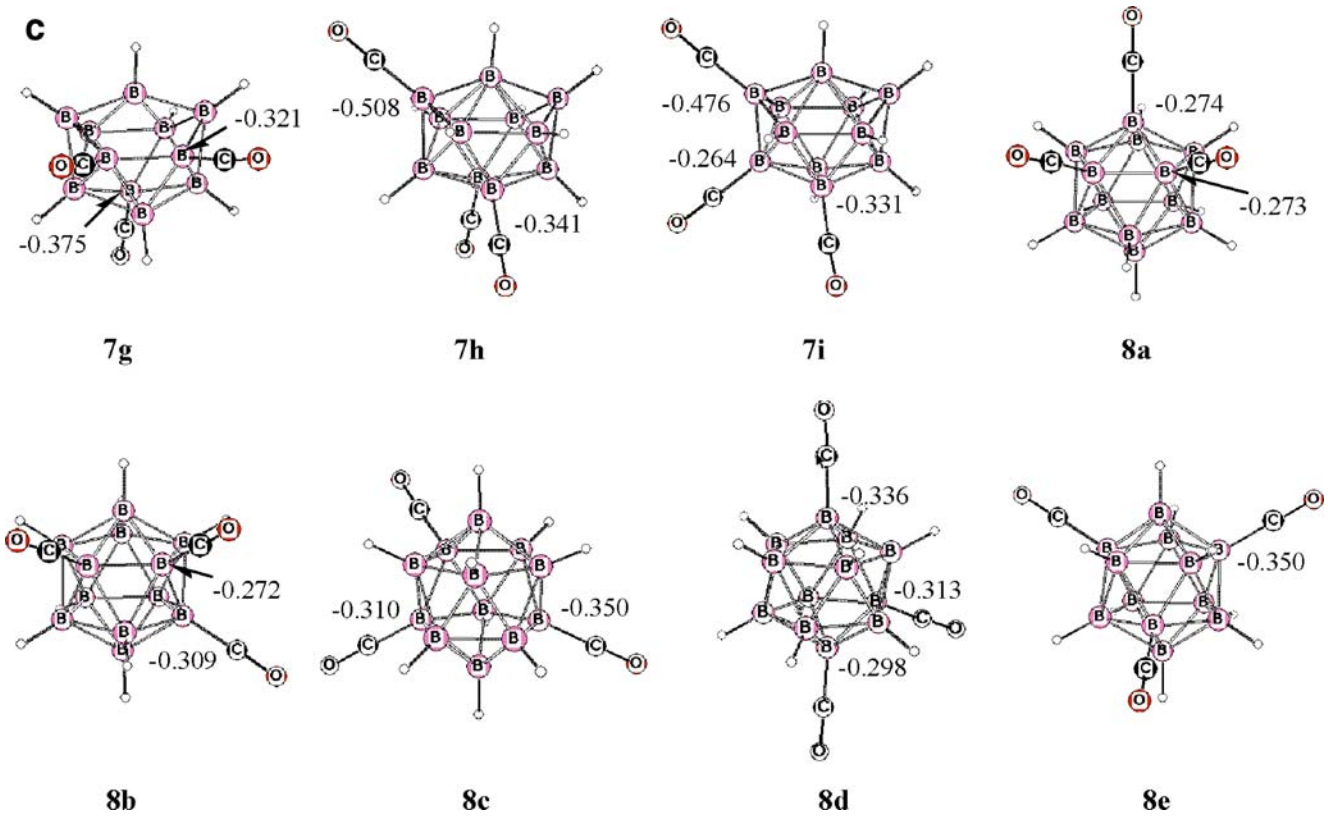

Fig. 1 (continued)

Closo-$B_9H_6(CO)_3^+$ (**5a–5j**): There are ten isomers for *closo*-$B_9H_6(CO)_3^+$, i.e., **5a** and **5g** in C_{3v} symmetry, **5b** in C_{2v} symmetry, **5c**, **5d**, **5h** and **5i** in C_1 symmetry, **5e** and **5f** in C_s symmetry, and **5j** in C_2 symmetry. The most stable isomer is **5a**, and the other isomers are higher in energy by 7.6 (**5b**), 8.3 (**5c**), 12.2 (**5d**), 26.9 (**5e**), 23.4 (**5f**), 18.9 (**5g**), 15.0 (**5h**), 19.0 (**5i**) and 21.5 (**5j**) kcal mol^{-1}. As expected, **5a** with the least connectivity and the largest separated negative charge is the most stable isomer.

Closo-$B_{10}H_7(CO)_3^+$ (**6a–6l**): The lower symmetry of $B_{10}H_{10}^{2-}$ results in 12 positional isomers for *closo*-$B_{10}H_7(CO)_3^+$; i.e., **6a–6c** and **6g–6i** in C_s symmetry, **6d** and **6l** in C_{2v} symmetry, as well as **6e**, **6f**, **6j** and **6k** in C_1, respectively. Among them, **6l** is the most stable isomer, and more stable than the second most stable isomer **6g** by 4.1 kcal mol^{-1}. It is to note that the most stable isomer **6l** has higher connectivity than the second most stable isomer **6g**, but **6l** has larger separated negative charge than **6g**. However, this energetic order is in contrast to that of *closo*-$C_3B_7H_{10}^+$, where **6g** is more stable than **6l** by 5.1 kcal mol^{-1}. The other isomers are higher in energy than **6l** by 23.1 (**6a**), 21.3 (**6b**), 17.3 (**6c**), 19.6 (**6d**), 7.5 (**6e**), 14.4 (**6f**), 4.8 (**6h**), 7.8 (**6i**), 15.2 (**6j**) and 11.0 (**6k**) kcal mol^{-1}, respectively.

Closo-$B_{11}H_8(CO)_3^+$ (**7a–7i**): There are nine isomers for *closo*-$B_{11}H_8(CO)_3^+$, i.e. **7a**, **7d** and **7i** in C_1 symmetry, **7b**, **7c** and **7e–7h** in C_s symmetry. The most stable isomer is **7c**, and the other isomers are higher in energy by 14.4 (**7a**), 6.1 (**7b**), 9.6 (**7d**), 8.8 (**7e**), 8.8 (**7f**), 7.9 (**7g**), 9.1 (**7h**) and 18.7 (**7i**) kcal mol^{-1}. Although the most stable and second most stable isomers **7c** and **7b** have the same connectivity, **7c** is much more stable than **7b**, and this is mainly due to the larger charge separation in **7c** than in **7b**.

Closo-$B_{12}H_9(CO)_3^+$ (**8a–8e**): Five isomers for *closo*-$B_{12}H_9(CO)_3^+$ are found; **8a** and **8e** in C_{3v} symmetry, **8b**, **8c** and **8d** in C_s symmetry. The most stable isomer is **8e**, and the other isomers are higher in energy by 26.9 (**8a**), 18.7 (**8b**), 9.6 (**8c**) and 7.3 (**8d**) kcal mol^{-1}. All five isomers have the same connectivity, but **8e** as the most stable isomer has the largest separated negative charge.

It is interesting to compare the relative stability of *closo*-$B_nH_{n-3}(CO)_3^+$ and *closo*-$C_3B_{n-3}H_n^+$. As given in Table 1, the most stable positional isomer for each *closo*-$B_nH_{n-3}(CO)_3^+$ cluster is the same as *closo*-$C_3B_{n-3}H_n^+$, apart from *closo*-$B_8H_5(CO)_3^+$ and *closo*-$B_{10}H_7(CO)_3^+$, indicating the similarity of two cluster types. The most significant difference is that *closo*-$B_nH_{n-3}(CO)_3^+$ have much smaller relative energies than *closo*-$C_3B_{n-3}H_n^+$. For example, the relative energies of the *closo*-$C_3B_4H_7^+$ isomers span a range of almost 70 kcal mol^{-1}, while the spread of relative energies is much smaller (15 kcal mol^{-1}) for the *closo*-$B_7H_4(CO)_3^+$ system. These results suggest the possi-

Table 1 Relative energies (E_{rel}, kcal mol^{-1}) of *closo*-$B_nH_{n-3}(CO)_3^+$

species	Symm.	(x/y/z)[a]	E_{rel}	E_{rel}[b,c]	species	Symm.	(x/y/z)[a]	E_{rel}	E_{rel}[b,c]
closo-$B_5H_2(CO)_3^+$					*closo*-$B_{10}H_7(CO)_3^+$				
1a	D_{3h}	4/4/4	4.4	43.0	**6a**	C_s	4/5/5	23.1	52.3
1b	C_1	3/4/4	5.4	28.4	**6b**	C_s	5/5/5	21.3	63.9
1c	C_{2v}	3/3/4	0.0	0.0	**6c**	C_s	5/5/5	17.3	55.6
closo-$B_6H_3(CO)_3^+$					**6d**	C_{2v}	4/5/5	19.6	43.4
2a	C_{3v}	4/4/4	2.8	9.6	**6e**	C_1	4/5/5	7.5	19.0
2b	C_{2v}	4/4/4	0.0	0.0	**6f**	C_1	4/5/5	14.4	33.7
closo-$B_7H_4(CO)_3^+$					**6g**	C_s	4/4/5	4.1	0.0
3a	C_{2v}	4/5/5	15.1	69.5	**6h**	C_s	4/5/5	4.8	16.4
3b	C_s	4/4/5	14.7	51.5	**6i**	C_s	5/5/5	7.8	35.4
3c	C_s	4/4/5	5.7	34.6	**6j**	C_1	5/5/5	15.2	50.5
3d	C_{2v}	4/4/4	9.3	18.1	**6k**	C_1	5/5/5	11.0	39.3
3e	C_{2v}	4/4/4	0.0	0.0	**6l**	C_{2v}	4/5/5	0.0	5.1
closo-$B_8H_5(CO)_3^+$					*closo*-$B_{11}H_8(CO)_3^+$				
4a	C_s	4/4/5	16.2	44.3	**7a**	C_1	4/4/6	14.4	37.2
4b	C_s	4/5/5	11.3	48.1	**7b**	C_s	4/4/5	6.1	13.7
4c	C_s	5/5/5	15.6	54.7	**7c**	C_s	4/4/5	0.0	0.0
4d	C_s	4/5/5	10.5	45.5	**7d**	C_1	4/5/5	9.6	31.8
4e	C_1	4/4/5	0.0	9.9	**7e**	C_s	4/5/5	8.8	31.8
4f	C_1	4/5/5	10.5	0.0	**7f**	C_s	5/5/5	8.8	40.2
4g	C_s	4/4/5	16.4	41.6	**7g**	C_s	5/5/5	7.9	38.1
4h	C_s	4/4/4	0.3	0.0	**7h**	C_s	4/5/5	9.1	80.5
4i	C_1	4/4/5	8.1	30.5	**7i**	C_1	4/5/5	18.7	49.8
closo-$B_9H_6(CO)_3^+$					*closo*-$B_{12}H_9(CO)_3^+$				
5a	C_{3v}	4/4/4	0.0	0.0	**8a**	C_{3v}	5/5/5	26.9	48.1
5b	C_{2v}	4/5/5	7.6	49.0	**8b**	C_s	5/5/5	18.7	32.5
5c	C_1	4/4/5	8.3	31.8	**8c**	C_s	5/5/5	9.6	16.2
5d	C_1	4/5/5	12.2	54.7	**8d**	C_s	5/5/5	7.3	13.3
5e	C_s	4/5/5	26.9	82.6	**8e**	C_{3v}	5/5/5	0.0	0.0
5f	C_s	4/5/5	23.4	63.3					
5g	C_{3v}	5/5/5	18.9	83.7					
5h	C_1	4/5/5	15.0	31.8					
5i	C_1	5/5/5	19.0	35.0					
5j	C_2	4/5/5	21.5	71.8					

a) Connectivity of BCO (or CH) units

b) Including the zero point energy, scaled by an empirical factor of 0.99.

c) Relative energies of *closo*-$C_3B_{n-3}H_n^+$ for comparison (ref [8], n=5, 6, 7, 10, 12 at B3LYP/6-31G* level) and n=8, 9 and 11 were calculated in this work at the same level.

bility that several of the *closo*-$B_7H_4(CO)_3^+$ isomers may be experimentally accessible.

It is also to note that there are energetic disorders for the less stable clusters of n=5, 7, 8, 9, 10 and 11 of *closo*-$C_3B_{n-3}H_n^+$ and *closo*-$B_nH_{n-3}(CO)_3^+$, but the relative energies for *closo*-$B_nH_{n-3}(CO)_3^+$ are much smaller than that of *closo*-$C_3B_{n-3}H_n^+$ (Table 1).

In addition to the relative stability of the individual cages, we have also computed the stability of the most stable cages as the function of their sizes. For that, we have used Eqs. (1) and (2) to evaluate the relative energies. The BH_{inc} increment in Eq. (1) is the energy difference between planer B_3H_5 and B_2H_4. The relative energy in Eq. (2) represents the strain energy difference between *closo*-$B_nH_{n-3}(CO)_3^+$ and *closo*-$C_3B_{n-3}H_n^+$. The computed reaction energies are given in Table 2.

$$2\,BCO + BCO^+ + (n-3)BH_{inc} \rightarrow B_nH_{n-3}(CO)_3^+ (n = 5-12) \quad (1)$$

$$C_3B_{n-3}H_n^+ + 3BH_3CO \rightarrow B_nH_{n-3}(CO)_3^+ + 3CH_4 (n = 5-12) \quad (2)$$

As given in Table 2, all calculated reaction energies (ΔH) by Eq. (1) and Eq. (2) are exothermic. Variations of

Table 2 Computed reaction energies (ΔH, kcal mol^{-1}), NICS values (ppm), C–O and C–B distances (Å), as well as the CO stretching frequencies (cm^{-1}) of the most stable *closo*-$B_nH_{n-3}(CO)_3^+$ (n=5−12) isomers as well as BH_3CO and $(CF_3)_3BCO$

Species	Symm	ΔH^a	ΔH^b	NICS[c]	C–O	C–B	ν_1[d]	ν_2[d]	ν_3[d,e]
1c	C_{2v}	−302.3	−61.2	−20.38	1.127	1.487	2178	2179	2216
2b	C_{2v}	−316.2	−74.6	−23.12	1.124	1.499	2184	2197	2225
3e	C_{2v}	−308.0	−52.9	−21.12	1.124	1.499	2191	2202	2219
4e	C_1	−290.1	−64.2	−18.66	1.125	1.504	2183	2192	2210
5a	C_{3v}	−291.8	−39.9	−20.55	1.124	1.505	2198	2198	2219
6l	C_{2v}	−294.8	−73.4	−25.85	1.123	1.512	2199	2205	2220
7c	C_s	−273.0	−57.7	−23.97	1.123	1.514	2200	2207	2222
8e	C_{3v}	−311.3	−85.0	−24.49	1.121	1.530	2219	2219	2231
BH_3CO	C_{3v}				1.131	1.521	2179		
$(CF_3)_3BCO$	C_3				1.119	1.589	2262		

a) On the basis of Eq. (1)
b) On the basis of Eq. (2)
c) At the cage center
d) Scaled by the factor (0.97) as the ratio between the computed and experimental detected CO frequency.
e) IR inactive mode, the relative IR intensities shown in Supporting Information

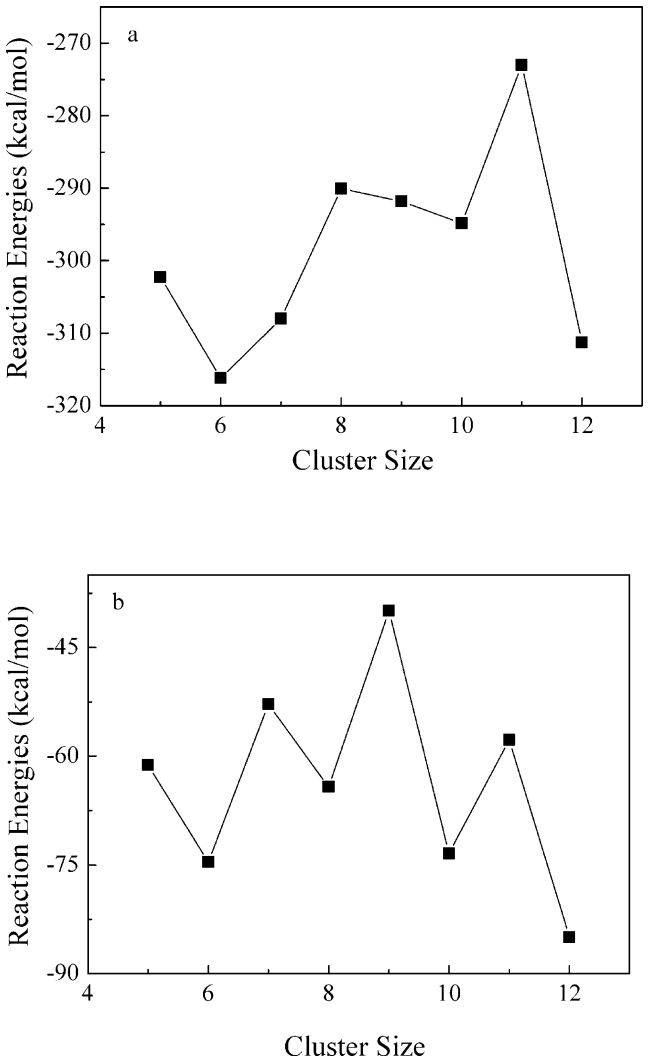

Fig. 2 (**a**) Plot of the reaction energies, of the most stable *closo*-$B_nH_{n-3}(CO)_3^+$ calculated by Eq. (1) vs. cluster size. (**b**) Plot of the reaction energies calculated by Eq. (2) vs. cluster size

individual compounds are apparent when the reaction energies (ΔH) are plotted as a function of the cluster size (Fig. 2). The plot is based on the data treatment employed previously to evaluate the relative stability of *closo*-$B_nH_n^{2-}$, *closo*-$CB_{n-1}H_n^-$ and *closo*-$C_2B_{n-2}H_n$ [7]. The reaction energies of *closo*-$B_nH_{n-3}(CO)_3^+$ calculated by Eq. (1) as a function of the cluster size is shown in Fig. 2a. It is found that the relative stability of *closo*-$B_nH_{n-3}(CO)_3^+$ evidently fluctuates as the size of the cluster increased, and clusters with n=6, 10 and 12 have larger relative stabilities. Their enhanced stability suggests the possibility for experiments.

The reaction energies of *closo*-$B_nH_{n-3}(CO)_3^+$ calculated by Eq. (2) represents strain energy differences between *closo*-$B_nH_{n-3}(CO)_3^+$ and *closo*-$C_3B_{n-3}H_n^+$. The values of these reaction energies are exothermic, indicating that *closo*-$B_nH_{n-3}(CO)_3^+$ is less strained than *closo*-$C_3B_{n-3}H_n^+$. These phenomena are found for $(BCO)_n$ and $(CH)_n$ cages [15]. The reaction energy of *closo*-$B_nH_{n-3}(CO)_3^+$ calculated by Eq. (2) as a function of cluster size is shown in Fig. 2b. It is found that the reaction energy fluctuates as the size of the cluster increased, and evidently clusters with n=6, 8, 10 and 12 have larger relative stabilities in this system, suggesting these clusters have the least strain energies compared with the corresponding closo-$C_3B_{n-3}H_n^+$ clusters.

Apart from the results of *closo*-$C_3B_{n-3}H_n^+$ (n=5, 6, 7, 10, 12) by Jemmis, we have computed the isomers for n=8, 9, 11. All results are given in Table S2 of Supporting Information. For *closo*-$C_3B_5H_8^+$, isomer **4h** with the least connectivity is most stable, while the other isomers are higher in energy by 44.3(**4a**), 48.1 (**4b**), 54.7 (**4c**), 45.5 (**4d**), 9.9 (**4e**), 41.6 (**4g**) and 30.5 (**4i**) kcal mol^{-1}. However, **4c**, **4d** and **4g** has one imaginary frequency and reduction of the C_s symmetry to C_1 results in local minimum, and **4c**,

4d and **4g** convert to **4e**, **4h** and **4i**, respectively In addition, isomer **4f** in C_1 symmetry converts directly to **4h** during the optimization.

Calculation on all the positional isomers of *closo*-$C_3B_6H_9^+$ identifies **5a** with the least connectivity is most stable, and the other isomers are higher in energy by 49.0 (**5b**), 31.8 (**5c**), 54.7 (**5d**), 82.6 (**5e**), 63.3 (**5f**), 83.7 (**5g**), 35.0 (**5i**) and 71.8 (**5g**) kcal mol^{-1}. Isomer **5h** with C_1 symmetry converts directly to **5c** during the optimization.

Among all the positional isomers of *closo*-$C_3B_8H_{11}^+$, **7c** with the least connectivity and the largest separation of the CH groups is most stable; the other isomers are higher in energy by 37.2 (**7a**), 13.7 (**7b**), 31.8 (**7d**), 31.8 (**7e**), 40.2 (**7f**), 38.1 (**7g**), 80.5 (**7h**) and 49.8 (**7i**) kcal mol^{-1}. All *closo*-$C_3B_{n-3}H_n^+$ calculated has qualitatively the same polyhedral structural pattern and the same number of positional isomers as *closo*-$B_nH_{n-3}(CO)_3^+$.

(b) **Aromaticity and CO stretching frequencies of *closo*-$B_nH_{n-3}(CO)_3^+$**

For characterizing the aromaticity of *closo*-$B_nH_{n-3}(CO)_3^+$, we used the computed NICS values at the cage center. For simplicity, we have chosen only the most stable positional isomer of individual cages in Table 1. The computed NICS values are given in Table 2.

As expected, *closo*-$B_nH_{n-3}(CO)_3^+$ have negative NICS values at the cage center, and $B_{10}H_7(CO)_3^+$ (**6l**) has the most negative NICS value (−25.9 ppm), followed by $B_{12}H_9(CO)_3^+$ (**8e**, −24.9 ppm). **2b** has also comparably large negative NICS value (−23.1 ppm). Therefore, it is generally to conclude that the most stable isomers of *closo*-$B_nH_{n-3}(CO)_3^+$ have also large negative NICS values. NICS values characterize the three-dimensional aromaticity of *closo*-$B_nH_{n-3}(CO)_3^+$ (n=5−12).

To aid experimental investigations, we have computed the CO stretching frequencies for all *closo*-$B_nH_{n-3}(CO)_3^+$ isomers, and these data are given in Supporting Information. For discussion, we present only those frequencies of the most stable isomers in Table 2, from which it is known that all the *closo*-$B_nH_{n-3}(CO)_3^+$ species have higher C–O stretching frequencies than 2143 cm^{-1}, the value for gaseous CO (the same is also found for other less stable isomers). In addition, the calculated CO stretching frequencies of BH_3CO and $(CF_3)_3BCO$ are given in Table 2 for comparison.

The characteristic feature for all known boron carbonyls (Table 2) is that the observed CO stretching frequencies are at higher wave numbers than CO [26, 27]. For most transition metal carbonyls, the CO stretching frequencies are lower than CO and this is explained by the strong back donation from transition metal into the CO π* orbital, [28] while for some transition metal carbonyls the observed CO stretching frequencies are at higher wave numbers than gaseous CO, and this is suggested as "nonclassical carbonyl", [29–31] in which metal → CO π back donation is indeed negligible and that the bonding is mainly due to OC → metal σ donation along with electrostatic attraction. This is particularly true when the metal is positively charged [32, 33]. Highly charged metal carbonyls may have strong bonds in spite of having little metal → CO π back donation, because the acceptor orbitals at the metal are energetically low lying and the additional Coulomb attraction is rather strong [28]. The electron deficiency of boron atom and the cationic character of *closo*-$B_nH_{n-3}(CO)_3^+$ cages make the Coulomb attraction stronger, leading to the rather high CO stretching frequencies.

The computed C–O and C–B distances are also included. For the most stable cages, the C–O distance increases, and the C–B distance decreases as the cage size decreases. The computed CO stretching frequencies decreases as the increased C–O distance along the decreased cage size.

Conclusions

The structure, stability and aromaticity of *closo*-$B_nH_{n-3}(CO)_3^+$ (n=5−12), which is isolobal with *closo*-$C_3B_{n-3}H_n^+$, have been investigated at the B3LYP/6−311+G** level of theory. The most stable positional isomers of individual clusters are obtained. The geometric pattern of the most stable positional isomer for each *closo*-$B_nH_{n-3}(CO)_3^+$ cluster is the same as *closo*-$C_3B_{n-3}H_n^+$, apart from *closo*-$B_8H_5(CO)_3^+$ and *closo*-$B_{10}H_7(CO)_3^+$.

Energetic analysis identifies *closo*-$B_6H_3(CO)_3^+$ (**2b**), *closo*-$B_{10}H_7(CO)_3^+$ (**6l**), and *closo*- $B_{12}H_9(CO)_3^+$ (**8e**) to have the largest relative stability, and should be the target for experimental investigation. It is found that *closo*-$B_nH_{n-3}(CO)_3^+$ cages are less strained than their *closo*-$C_3B_{n-3}H_n^+$ counterparts based on the negative reaction energies calculated by Eq. (2).

The computed negative NICS values identify *closo*-$B_nH_{n-3}(CO)_3^+$ as aromatic compounds. To aid experimental investigations, C–O stretching frequencies were calculated. The absence of π-back donation and electrostatic attraction in the B–CO interactions should be responsible for this "non-classical carbonyl".

Acknowledgments This work was supported by the National Nature Science Foundation of China (20471034).

References

1. Hawthorne MF (1993) Angew Chem Int Ed Engl 32:950–984
2. Bregadze VI (1992) Chem Rev 92:209–223
3. Grimes RN (1998) Carboranes, anti-crowns, big wheels, and super-sandwiches. In: Mulzer J, Waldmann H (eds) Organic synthesis highlights III. Wiley-VCH, pp 406–414

4. Dewar MJS, McKee ML (1980) Inorg Chem 19:2662–2672
5. Gimarc BM, Zhao M (1996) Inorg Chem 35:825–834
6. Ott JJ, Gimarc BMJ (1986) Comput Chem 7:673–692
7. Schleyer PvR, Najafian K (1998) Inorg Chem 37:3454–3470
8. Jemmis ED, Ramalingam M, Jayasree EGJ (2001) Comput Chem 22:1542–1551
9. Hoffmann R (1982) Angew Chem Int Ed Engl 21:711–717
10. Zhou M, Wang ZX, Schleyer PvR (2003) ChemPhysChem 4:763–766
11. Papakondylis A, Miliordos E, Mavridis A (2004) J Phys Chem A 108:4335–4340
12. Burg BA, Schlesinger HI (1937) J Am Chem Soc 59:780–787
13. Zhou M, Xu Q, Wang ZX, Schleyer PvR (2002) J Am Chem Soc 124:14854–14855
14. Wu HS, Jiao H, Wang ZX, Schleyer PvR (2003) J Am Chem Soc 125:4428–4429
15. Wu HS, Qin XF, Xu XH, Jiao H, Schleyer PvR (2005) J Am Chem Soc 127:2334–2338
16. Wang ZX, Chen ZF, Jiao H, Schleyer PvR (2005) J Theo Comp Chem 4:669–688
17. Schleyer PvR, Maerker C, Dransfeld A, Jiao H, vE Hommes NJR (1996) J Am Chem Soc 118:6317–6318
18. Schleyer PvR, Jiao H, vE Hommes NJR, Malkin VG, Malkina OL (1997) J Am Chem Soc 119:12669–12670
19. Schleyer PvR, Manoharan M, Wang ZX, Kiran B, Jiao H, Puchta R, vE Hommes NJR (2001) Org Lett 3:2465–2468
20. Wolinski K, Hinton JF, Pulay P (1990) J Am Chem Soc 112:8251–8260
21. Frisch MJ et al (2003) Gaussian, Inc., Pittsburgh PA
22. Williams RE (1976) Adv Inorg Chem Radiochem 18:67–142
23. Wade K (1971) Chem Commun 792–793
24. Ott JJ, Gimarc BM (1986) J Am Chem Soc 108:4303–4308 and references cited therein
25. Jemmis ED (1982) J Am Chem Soc 104:7017–7020
26. Finze M, Berndhardt E, Terheiden A, Berkei M, Wilner H, Christen D, Oberhammer H, Aubke F (2002) J Am Chem Soc 124:15385–15398 and references therein
27. Hehre WJ, Randon L, Schleyer PvR, Pople JA (1986) Ab initio molecular orbital theory. Wiley, New York
28. Szilagyi R, Frenking G (1997) Organometallics 16:4807–4815
29. Strauss SH (1997) Chemtracts Inorg Chem 10:77–103
30. Lupinetti AJ, Frenking G, Strauss SH (1998) Angew Chem 110:2229–2232
31. Lupinetti AJ, Frenking G, Strauss SH (1998) Angew Chem Int Ed Engl 37:2113–2116
32. Goldman AS, Krogh-Jespersen K (1996) J Am Chem Soc 118:12159–12166
33. Ehlers AW, Ruiz-Morales Y, Baerends EJ, Ziegler T (1997) Inorg Chem 36:5031–5036